Archimedean Tiling Patterns of ABC Star-Shaped Terpolymers Studied by Microbeam Small-Angle X-ray Scattering

Kenichi Hayashida,[†] Wataru Kawashima,[†] Atsushi Takano,[†,⊥] Yuya Shinohara,[‡] Yoshiyuki Amemiya,[‡] Yoshinobu Nozue,[§] and Yushu Matsushita*[,†]

Department of Applied Chemistry, Graduate School of Engineering, Nagoya University, Nagoya 464-8603, Japan; Department of Advanced Materials Science, Graduate School of Frontier Sciences, University of Tokyo, Chiba 277-8561, Japan; Petrochemicals Research Laboratory, Sumitomo Chemical Co., Ltd., Kitasode, Japan; and Precursory Research for Embryonic Science and Technology (PRESTO), Japan Science and Technology Agency, 4-1-8 Honcho, Kawaguchi 332-0012, Japan

Received March 23, 2006; Revised Manuscript Received May 2, 2006

ABSTRACT: Characteristic cylindrical structures formed by ABC star-shaped terpolymers were investigated by microbeam small-angle X-ray scattering (SAXS) in addition to transmission electron microscopy (TEM). The polymer samples are composed of polyisoprene (I), polystyrene (S), and poly(2-vinylpyridine) (P); their volume ratios for I:S:P are 1:1:*X*, where *X* equals 0.7, 1.2, 1.3, and 1.9. The spotlike diffraction patterns were observed by microbeam SAXS due to scattering from a small number of ordered grains in the polymer samples, where the exact packing manners of the cylinders, or their lattice constants, have been clarified. In short, it has been found that the cross-sectional patterns of these tilings have the features of four Archimedean tiling patterns, i.e., (6.6.6), (4.8.8), (3.3.4.3.4), and (4.6.12). All the four SAXS patterns are quite consistent with the structural observation by TEM with regard to the crystallographic data.

Introduction

Block and graft copolymers with incompatible components are known to show periodic nanophase-separated structures at the condensed states due to strong repulsion forces interacting between different chemical components.[1−4] They give various morphologies, such as spherical, cylindrical, bicontinuous, and lamellar structures, depending on their volume fractions. Among the block copolymers, the ABC star-shaped terpolymers tend to form characteristic cylinder-based phase-separated structures since three different polymer components are connected at one junction point which must be aligned one-dimensionally due to the geometrical restriction.[5−15]

We have previously reported that the characteristic cylindrical structures were observed by transmission electron microscopy (TEM) for the ISP star-shaped terpolymers composed of polyisoprene (I), polystyrene (S), and poly(2-vinylpyridine) (P).[15] The cross sections of the cylindrical structures reveal periodic tiling patterns consisting of regular polygons, i.e., (6.6.6), (4.8.8), and (4.6.12), which are families of the 12 Archimedean tiling patterns.[16] Recently, a more complex Archimedean tiling pattern, (3.3.4.3.4), has also been found for the sample with exact compositions in the same ISP star-shaped terpolymer series.[17] At the same time, it has been clarified that the grain sizes of these structures are fairly small compared with those of linear block copolymers.

In addition to the TEM observation, the small-angle X-ray scattering (SAXS) technique should be used to determine the structural features of the various cylindrical structures precisely in the reciprocal lattice space. However, in the conventional SAXS measurements, the typical size of X-ray beam is about 0.5 mm × 0.5 mm or larger, which is much larger than the average grain sizes of the cylindrically ordered nanoscopic structures for the present ABC star-shaped terpolymers. Therefore, the resultant two-dimensional SAXS patterns consist of the reflections from a large number of grains rotated randomly around the [001] direction (the cylindrical axis). Accordingly, the observed two-dimensional patterns are powder patterns rather than the desirable spotlike reflections with the corresponding symmetry. This fact has made it difficult to characterize the tiling patterns from the complex molecules such as the star-branched copolymers used in the present study by conventional SAXS measurements.

On the other hand, the microbeam SAXS technique has been developed recently to observe nanoscopic structures in polymeric materials.[18−24] Among them, Dreher et al. reported the microstructure of liquid crystalline polymer samples.[18] These samples showed isotropic scattering patterns when examined by conventional SAXS measurement (the beam size was 2 mm in diameter), while local variations of the molecular orientation in liquid crystalline polymer sample were observed by microbeam SAXS system (the beam size was 7 μm in diameter). Furthermore, the microbeam SAXS techniques were used to study the organization in single fibers,[19−21] the local arrangement of the smectic layers in poly(ester imide)s,[22] the kinetics of secondary crystallization of polymeric materials,[23] the structural inhomogeneity within the band spherulite of the miscible polymer blends,[24] and so on. Thus, the microbeam SAXS techniques would be powerful to obtain nanoscopic structural information within the macroscale polymer samples.

In this work, therefore, the cylindrical structures having the features of the Archimedean tiling patterns formed by the ABC star-shaped terpolymers were investigated by microbeam SAXS. The microbeam SAXS patterns are analyzed in comparison with the results of the TEM observations in order to elucidate the structural features of the present terpolymers accurately in the crystallographic sense.

[†] Nagoya University.
[‡] University of Tokyo.
[§] Sumitomo Chemical Co., Ltd.
[⊥] PRESTO, Japan Science and Technology.
* To whom all correspondence should be addressed: Tel +81-52-789-4605; Fax +81-52-789-3210; e-mail yushu@apchem.nagoya-u.ac.jp.

10.1021/ma060647p CCC: $33.50
Published on Web 06/07/2006

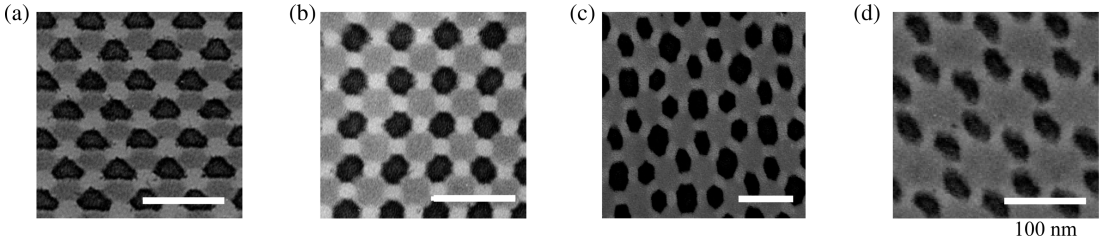

Figure 1. TEM images of the four star-shaped terpolymer samples: $I_{1.0}S_{1.0}P_{0.7}$ (a), $I_{1.0}S_{1.0}P_{1.2}$ (b), $I_{1.0}S_{1.0}P_{1.3}$ (c), and $I_{1.0}S_{1.0}P_{1.9}$ (d).

Experimental Section

Three polymer samples composed of polyisoprene (I), polystyrene (S), and poly(2-vinylpyridine) (P) were synthesized by anionic polymerizations.[15] Their volume ratios for I:S:P are 1:1:*X*, where *X* equals 0.7, 1.2, and 1.9; therefore, they were coded as $I_{1.0}S_{1.0}P_{0.7}$, $I_{1.0}S_{1.0}P_{1.2}$, and $I_{1.0}S_{1.0}P_{1.9}$, respectively. Another polymer sample with $X = 1.3$ was also prepared by blending two samples, i.e., $I_{1.0}S_{1.0}P_{1.2}$ and $I_{1.0}S_{1.0}P_{1.9}$, at the weight ratio of 0.85/0.15.[17]

Sample films were obtained by solvent casting from 2% solutions of the samples in tetrahydrofuran; successively, they were dried at room temperature for 6 h and annealed at 140 °C under a vacuum for a week.

For TEM observations, the annealed samples were stained with osmium tetroxide, which heavily stains I and intermediately does P, and cut into ultrathin sections with ca. 50 nm thickness using an ultramicrotome, Reica Ultracut FCS, at room temperature with a diamond knife (Diatome cryo-T). The TEM observations were carried out in the same manner reported previously.[25]

For microbeam SAXS measurements, the sample films were cut into thin sections with ca. 20 μm thickness, where the film edges are the observation angle using the same ultramicrotome system. The microbeam SAXS measurements were performed at high flux beamline BL40XU of SPring-8 (Hyogo, Japan) equipped with a helical undulator.[26] The wavelength of X-ray was 0.1 nm, and the size of the X-ray microbeam was ca. 5 μm × 5 μm (fwhm), which was obtained by merely inserting a pinhole of 3 μm in diameter at the upstream of the sample position. The parasitic scattering was removed by a second pinhole at the sample position. The camera length was fixed about 3 m, and the precise camera length was calibrated with a collagen standard sample. The polymer samples were placed at a sample stage which was controlled remotely from outside the experimental hutch and scanned with every 1−10 μm step in order to obtain the scattering patterns from ordered grains, the cylindrical axes of which were close to parallel to the incident beam. The scattering patterns were recorded with a cooled CCD detector coupled with an X-ray image intensifier (Hamamatsu Photonics Ltd., Japan).[27]

Results and Discussion

Figure 1 shows the TEM images of the four star-shaped terpolymer samples. Since the samples were stained with osmium tetroxide for the TEM observations, the black, white, and gray domains represent I, S, and P phases, respectively. $I_{1.0}S_{1.0}P_{0.7}$ shows a honeycomb-type structure consisting of three kinds of hexagonal domains which meet at every vertex, hence resulting in forming the (6.6.6) Archimedean tiling pattern.[15] In the same way, the domain packing manners of $I_{1.0}S_{1.0}P_{1.2}$ and $I_{1.0}S_{1.0}P_{1.9}$ are classified into (4.8.8) and (4.6.12) Archimedean tiling patterns, respectively. On the other hand, $I_{1.0}S_{1.0}P_{1.3}$ shows a complex tiling pattern, to which any simple tiling patterns apparently cannot be applied in a direct manner. Instead, the tiling pattern is found to be assigned as the (3.3.4.3.4) structure, which is another one of the Archimedean tiling patterns, by applying an indirect tiling manner.[17]

Figure 2 shows the microbeam SAXS pattern of $I_{1.0}S_{1.0}P_{0.7}$, and the corresponding tiling structure is schematically represented, where the white arrows denote the real lattice vectors,

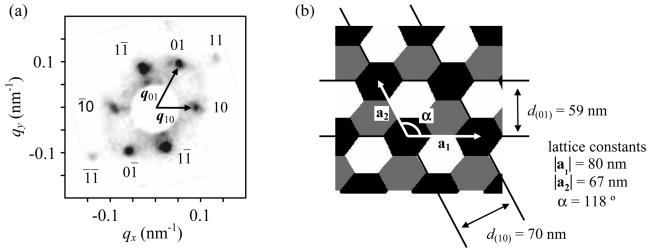

Figure 2. Microbeam SAXS pattern of $I_{1.0}S_{1.0}P_{0.7}$ (a) and the corresponding schematic tiling structure (b).

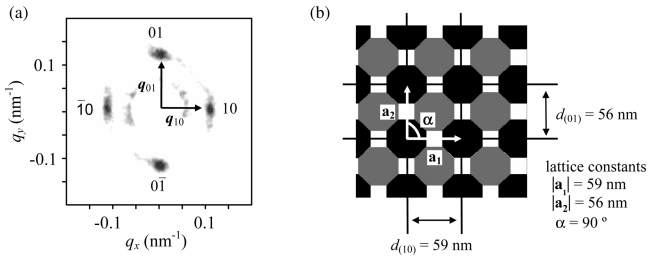

Figure 3. Microbeam SAXS pattern of $I_{1.0}S_{1.0}P_{1.2}$ (a) and the corresponding schematic tiling structure (b).

$\mathbf{a}_1$ and $\mathbf{a}_2$. In the SAXS pattern, spotlike reflections are observed, indicating that the X-ray beam size is small enough to probe only a limited number of grains ordered cylindrically in the sample film. The sizes of the grains are typically a few microns according to the TEM observations; therefore, the SAXS pattern should be obtained from a small number of grains. This SAXS pattern apparently shows six spots of first-order reflections, which is consistent with the (6.6.6) tiling pattern observed in Figure 1a. The *d*-spacings, or $d_{(10)}$ and $d_{(01)}$, in Figure 2b were estimated to be 70 and 59 nm from the magnitudes of the corresponding scattering vectors $|\mathbf{q}_{(10)}|$ and $|\mathbf{q}_{(01)}|$, respectively, designated in Figure 2a using the relationship $d = 2\pi/|\mathbf{q}|$. The angle between the two scattering vectors, 62°, gives the angle α, 118°, between the real lattice vectors. The *d*-spacings and the angle α, in turn, give the magnitudes of the real lattice vectors, $|\mathbf{a}_1|$ and $|\mathbf{a}_2|$, i.e., 80 and 67 nm, respectively, suggesting that the hexagonal lattice in real space is distorted as shown in Figure 2b. In fact, the hexagonal structure observed by TEM (Figure 1a) is a little more distorted than the structure model in Figure 2b. In addition, this distortion would cause the difference in the intensities of the first-order reflections in Figure 2a.

Figure 3 illustrates the microbeam SAXS pattern of $I_{1.0}S_{1.0}P_{1.2}$ and the corresponding tiling structure. The SAXS pattern shows a 4-fold symmetry, which is consistent with the (4.8.8) tiling pattern having the square lattice for this sample. The 10 reflections located on the meridian and the equator suggest the actual lattice for $I_{1.0}S_{1.0}P_{1.2}$ is rectangular as shown in Figure 3b. The *d*-spacings and the lattice constants for this square lattice were determined in the same manner as for $I_{1.0}S_{1.0}P_{0.7}$ in Figure 2, and they are as follows: $d_{(10)} = |\mathbf{a}_1| = 59$ nm, $d_{(01)} = |\mathbf{a}_2| = 56$ nm, $\alpha = 90°$. It is apparent that the crystallographic data in Figure 3b agree well with those observed in Figure 1b.

Table 1. Two-Dimensional Lattice Constants for the Cylindrical Structures for the Star-Shaped Terpolymer Samples Obtained from the SAXS Patterns and the TEM Observations

sample	microbeam SAXS results	TEM results	structure
$I_{1.0}S_{1.0}P_{0.7}$	$\|\mathbf{a}_1\| = 80$ nm, $\|\mathbf{a}_2\| = 67$ nm, $\alpha = 118°$	$\|\mathbf{a}_1\| = 63$ nm, $\|\mathbf{a}_2\| = 47$ nm, $\alpha = 131°$	(6.6.6)
$I_{1.0}S_{1.0}P_{1.2}$	$\|\mathbf{a}_1\| = 59$ nm, $\|\mathbf{a}_2\| = 56$ nm, $\alpha = 90°$	$\|\mathbf{a}_1\| = 53$ nm, $\|\mathbf{a}_2\| = 53$ nm, $\alpha = 92°$	(4.8.8)
$I_{1.0}S_{1.0}P_{1.3}$	$\|\mathbf{a}_1\| = 150$ nm, $\|\mathbf{a}_2\| = 146$ nm, $\alpha = 105°$	$\|\mathbf{a}_1\| = 230$ nm, $\|\mathbf{a}_2\| = 190$ nm, $\alpha = 103°$	(3.3.4.3.4)
$I_{1.0}S_{1.0}P_{1.9}$	$\|\mathbf{a}_1\| = 98$ nm, $\|\mathbf{a}_2\| = 90$ nm, $\alpha = 123°$	$\|\mathbf{a}_1\| = 90$ nm, $\|\mathbf{a}_2\| = 86$ nm, $\alpha = 131°$	(4.6.12)

Figure 4 shows the microbeam SAXS pattern and the tiling structure of $I_{1.0}S_{1.0}P_{1.3}$. In the SAXS pattern, the 20 and 21 reflections are clearly observed in addition to the 11 reflections, which are characteristic for the (3.3.4.3.4) tiling pattern. Although the right (3.3.4.3.4) structure composed of equilateral triangles and squares should be a square lattice, the reflections in the SAXS pattern are located on a parallelogram instead, indicating that the real lattice for $I_{1.0}S_{1.0}P_{1.3}$ is considerably distorted, resulting in forming an oblique lattice. The lattice constants were determined to be 150 nm for $|\mathbf{a}_1|$, 146 nm for $|\mathbf{a}_2|$, and 105° for α. Comparing Figure 4b and Figure 1c, the degree of the distortion of the lattice is quite consistent with each other.

Figure 5 illustrates the microbeam SAXS pattern and the tiling structure of $I_{1.0}S_{1.0}P_{1.9}$. The SAXS pattern in Figure 5a shows a 6-fold scattering symmetry, which is consistent with the (4.6.12) tiling pattern observed in Figure 1d, though the SAXS pattern is also deformed to lead the imperfect hexagonal lattice ($|\mathbf{a}_1| = 98$ nm, $|\mathbf{a}_2| = 90$ nm, $\alpha = 123°$) for this tiling.

Table 1 summarizes the lattice constants for the cylindrical structures for the star-shaped terpolymer samples obtained from the SAXS patterns and the TEM observations. The sizes of the lattices obtained from the SAXS results are fairly different from those from the TEM results for $I_{1.0}S_{1.0}P_{0.7}$ and $I_{1.0}S_{1.0}P_{1.3}$. It is suggested that the considerable difference in dimensions between the TEM and SAXS results is mainly attributed to the inaccuracy in the magnification of the TEM observations. The magnification of TEM images are sensitive to conditions for taking micrographs while the scales of the SAXS patterns could be more accurate since the camera length adopted was calibrated with the standard sample. In addition, it is difficult to observe the right cross sections of the cylindrical structures perpendicular to the cylindrical axes by TEM. This fact causes the difference not only in the sizes of the lattices but also in the angles α between the TEM and SAXS results. Moreover, it is apparent that the two experiments were observing just one or small number of grains at different locations, so that the lattice constants can vary.

In conclusion, it has been found that the microbeam SAXS measurements give the spotlike diffraction patterns, which were never obtained by conventional SAXS measurements, due to scattering from a small number of ordered grains in the polymer samples. These SAXS patterns are quite consistent with the structural observation by TEM with regard to the symmetry of four Archimedean tiling patterns, i.e., (6.6.6), (4.8.8), (3.3.4.3.4), and (4.6.12). It has been also confirmed that the real lattices formed by the star-shaped terpolymer samples are actually distorted to some extent in comparison with the ideal lattice for the tiling structures. The lattice constants for the distorted periodic tiling patterns have been successfully determined, so that the packing manners of cylinders for the present ISP star-shaped terpolymers have been clarified quantitatively by the microbeam SAXS technique adopted.

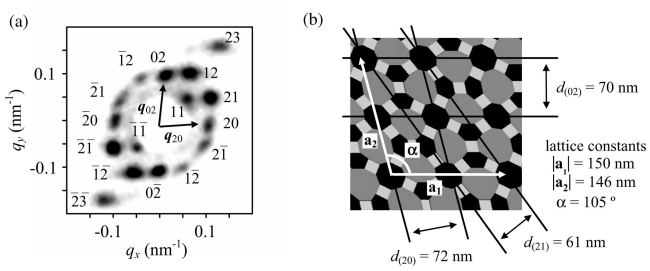

Figure 4. Microbeam SAXS pattern of $I_{1.0}S_{1.0}P_{1.3}$ (a) and the corresponding schematic tiling structure (b).

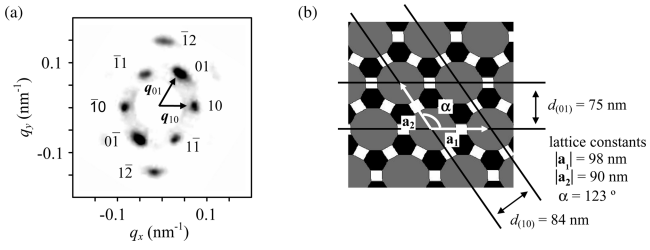

Figure 5. Microbeam SAXS pattern of $I_{1.0}S_{1.0}P_{1.9}$ (a) and the corresponding schematic tiling structure (b).

Acknowledgment. We greatly thank Dr. S. Arai at the Ecotopia Science Institute in Nagoya University for his help in taking transmission electron micrographs. This work was partially supported by a research grant from the 21st century COE program under support from the Japan Society for the Promotion of Science (JSPS) entitled "Nature-Guided Materials Processing" in the School of Engineering, Nagoya University, and K.H. and Y.M. are thankful for the program. This work was also partly supported by a grant from PRESTO, Japan Science and Technology Corporation (JST), and A.T. is thankful for the support. The SAXS experiments were performed under the approval of SPring-8 (Proposal No. 2005A0221 and 2005B0155).

References and Notes

(1) Molau, G. E. In *Block Copolymers*; Agarwal, S. L., Ed.; Plenum Publishing: New York, 1970.
(2) Norshay, A.; McGrath, J. E. Block Copolymers. In *Overview and Critical Survey*; Academic Press: New York, 1977.
(3) Riess, G. *Encyclopedia of Polymer Science and Engineering*; John Wiley & Sons: New York, 1986.
(4) Galllot, B. R. M. *Adv. Polym. Sci.* **1978**, *29*, 85.
(5) Fujimoto, T.; Zhang, H.; Kazama, T.; Isono, Y.; Hasegawa, H.; Hashimoto, T. *Polymer* **1992**, *33*, 2208.
(6) Iatrou, H.; Hadjichristidis, N. *Macromolecules* **1992**, *25*, 4649.
(7) Hadjichristidis, N.; Iatrou, H.; Behal, S. K.; Chludzinski, J. J.; Disko, M. M.; garner, R. T.; Liang, K. S.; Lohse, D. J.; Milner, S. T. *Macromolecules* **1993**, *26*, 5812.
(8) Okamoto, S.; Hasegawa, H.; Hashimoto, T.; Fujimoto, T.; Zhang, H.; Kazama, T.; Takano, A.; Isono, Y. *Polymer* **1997**, *38*, 5275.
(9) Sioula, S.; Tselikas, Y.; Hadjichristidis, N. *Macromolecules* **1997**, *30*, 1518.
(10) Sioula, S.; Hadjichristidis, N.; Thomas, E. L. *Macromolecules* **1998**, *31*, 5272.
(11) Sioula, S.; Hadjichristidis, N.; Thomas, E. L. *Macromolecules* **1998**, *31*, 8429.
(12) Huckstadt, H.; Gopfert, A.; Abetz, V. *Macromol. Chem. Phys.* **2000**, *201*, 296.

(13) Bellas, V.; Iatrou, H.; Hadjichristidis, N. *Macromolecules* **2000**, *33*, 6993.
(14) Yamauchi, K.; Takahashi, K.; Hasegawa, H.; Iatrou, H.; Hadjichristidis, N.; Kaneko, T.; Nishikawa, Y.; Jinnai, H.; Matsui, T.; Nishioka, H.; Shimizu, M.; Furukawa, H. *Macromolecules* **2003**, *36*, 6962.
(15) Takano, A.; Wada, S.; Sato, S.; Araki, T.; Hirahara, K.; Kazama, T.; Kawahara, S.; Isono, Y.; Ohno, A.; Tanaka, N.; Matsushita, Y. *Macromolecules* **2004**, *37*, 9941.
(16) Grunbaum, B.; Shephard, G. C. In *Tilings and Patterns*; Freeman: New York, 1986.
(17) Takano, A.; Kawashima, W.; Noro, A.; Isono, Y.; Tanaka, N.; Dotera, T.; Matsushita, Y. *J. Polym. Sci., Part B: Polym. Phys.* **2005**, *43*, 2427.
(18) Dreher, S.; Zachmann, H. G.; Riekel, C.; Engstrom, P. *Macromolecules* **1995**, *28*, 7071.
(19) Mullar, M.; Czihak, C.; Vogl, G.; Fratzl, P.; Schober, H.; Riekel, C. *Macromolecules* **1998**, *31*, 3953.
(20) Ohta, N.; Oka, T.; Inoue, K.; Yagi, N.; Kato, S.; Hatta, I. *J. Appl. Crystallogr.* **2005**, *38*, 274.
(21) Kajiura, Y.; Watanabe, S.; Itou, T.; Iida, A.; Shinohara, Y.; Amemiya, Y. *J. Appl. Crystallogr.* **2005**, *38*, 420.
(22) Gurke, I.; Wutz, C.; Gieseler, D.; Janssens, B.; Heidelbach, F.; Riekel, C.; Kricheldorf, H. R. *J. Appl. Crystallogr.* **2000**, *33*, 718.
(23) Kolb, R.; Wutz, C.; Stribeck, N.; von Krosigk, G.; Riekel, C. *Polymer* **2001**, *42*, 5257.
(24) Nozue, Y.; Kurita, R.; Hirano, S.; Kawasaki, N.; Ueno, S.; Iida, A.; Nishi, T.; Amemiya, Y. *Polymer* **2003**, *44*, 6397.
(25) Matsushita, Y.; Iwata, H.; Asari, T.; Uchida, T.; ten Brinke, G.; Takano, A. *J. Chem. Phys.* **2004**, *121*, 1129.
(26) Inoue, K.; Oka, T.; Suzuki, T.; Yagi, N.; Takeshita, K.; Goto, S.; Ishikawa, T. *Nucl. Instrum. Methods* **2001**, *A467−469*, 674.
(27) Amemiya, Y.; Ito, K.; Yagi, N.; Asano, Y.; Wakabayashi, K.; Ueki, T.; Endo, T. *Rev. Sci. Instrum.* **1995**, *66*, 2290.

MA060647P